

In Vitro Assessment of Antibacterial Activity and Cytocompatibility of Silver-Containing PHBV Nanofibrous Scaffolds for Tissue Engineering

Zhi-Cai Xing,[†] Won-Pyo Chae,[†] Jin-Young Baek,[†] Moon-Jeong Choi,[‡] Yongsoo Jung,[§] and Inn-Kyu Kang^{*,†}

Departments of Polymer Science and Engineering and Medical and Biological Engineering, Kyungpook National University, Daegu 702-701, Korea, and Materials Processing Division, Korea Institute of Materials Science, Changwon 641-010, South Korea

Received January 13, 2010; Revised Manuscript Received March 7, 2010

Infections with bacteria have become a serious problem in joint arthroplasty. This study reports about in vitro antibacterial activity and in vitro cell compatibility of poly-(3-hydroxybutyrate-co-3-hydroxyvalerate) (PHBV) nanofibers loaded with metallic silver particles of a size of 5–13 nm. In vitro antibacterial activity against *Staphylococcus aureus* and *Klebsiella pneumoniae* was studied by microplate proliferation tests. The adhesion, viability, and proliferation properties of fibroblasts (NIH 3T3) and differentiation of osteoblasts (MC3T3-E1) were done to study in vitro cell compatibility of the scaffolds. As the results, only silver-containing PHBV nanofibrous scaffolds showed a high antibacterial activity and an inhibitory effect on the growth of both *Staphylococcus aureus* and *Klebsiella pneumoniae* bacteria. The nanofibrous scaffolds having silver nanoparticles <1.0% were free of in vitro cytotoxicity. To sum up, the PHBV nanofibrous scaffolds having nanoparticles <1.0 wt % showed not only good antibacterial activity but also good in vitro cell compatibility. It is considered that the PHBV nanofibrous scaffolds with silver nanoparticles <1.0 wt % have a potential to be used in joint arthroplasty.

Introduction

With the outbreaks of infectious diseases caused by pathogenic bacteria and the rise of antibiotic resistance of bacteria,¹ much attention in pharmaceutical and medical fields has been focused on creating new antibacterial agents.² Nanocrystalline silver has been proven to be the most effective antimicrobial agent³ as silver, and its compounds have powerful antimicrobial capability⁴ and broad inhibitory biocidal spectra for microbes including bacteria, viruses, and eukaryotic microorganisms.^{5–7} Enhanced antibacterial properties of nanocrystalline silver have been used in different fields in medicine for years, as Crede's prophylaxis for ophthalmia neonatorum,⁸ in wound healing,⁹ or in biomaterials.¹⁰ Relevant clinical cytotoxicity of silver has also been reported.^{11,12}

Poly-(3-hydroxybutyric acid-co-3-hydroxyvaleric acid) (PHBV) is a biodegradable and biocompatible polyester polymerized by bacteria.¹³ PHBV can be used for biomedical applications because of its biocompatibility and nontoxicity for living tissues. The biomedical applications mentioned in the literature include surgical suture, surgical swabs, wound dressings, vascular graft, blood vessels, and scaffolds for new tissue in growth and body parts.¹⁴

Ultrafine fiber scaffolds prepared by the electrospinning of a polymer solution have been extensively studied because of their unique properties such as high surface area-to-volume ratio. Recently, the incorporation of silver nanoparticles into ultrafine fibers has attracted a great deal of attention because the resulting

fibers have very strong antimicrobial activity. So far, silver-containing nanofibers, such as poly-(L-lactide),¹⁵ activated carbon,¹⁶ polypropylene,¹⁷ nylon 6,¹⁸ and PMMA¹⁹ have been electrospun successfully, and their antibacterial activity has been observed. However, to date, no report has yet been published showing the antibacterial activity and cytotoxicity of silver containing-PHBV nanofibrous scaffolds by electrospinning.

The purpose of this study is to evaluate the potential of PHBV nanofibers loaded with silver particles of a size of 5–13 nm as tissue engineering scaffolds. To achieve the purpose, the antibacterial activity of PHBV nanofibrous scaffolds with different amount of silver against *Staphylococcus aureus* and *Klebsiella pneumoniae* was studied. Furthermore, the in vitro cytocompatibility of the scaffolds was also investigated.

Materials and Methods

Preparation of Polymer Solution. PHBV (hydroxyvaleric acid content: 5 wt %; Aldrich Chemical) was dissolved in 2,2,2-trifluoroethyl alcohol at a concentration of 5 wt %, and the solution was stirred overnight at room temperature to ensure complete dissolution. Then, certain amounts of silver nanoparticles (0.1 to 1 wt %, the percentage of silver nanoparticles to PHBV; Hunion Co., Korea) were mixed with PHBV solution and stirred by magnetic stirring for 24 h to get the silver-containing PHBV solution. The solution was further homogenized with ultrasonic for 2 h and then subjected to the electrospinning experiments.

Electrospinning. The electrospinning experiments were performed at room temperature, and the apparatus for the electrospinning was assembled based on the study carried out by Lee et al.²⁰ The polymer solution was placed in a 10 mL glass syringe fitted with a needle (20 G). A clamp connected to a high voltage power supply, which could supply a positive voltage from 0 to 50 kV, was attached to the needle. A piece of aluminum foil was placed at a distance of 15 cm apart from the needle tip. The polymer jets generated from the needle by high

* To whom correspondence should be addressed. Tel: +82 53 950 5629. Fax: +82 53 950 6623. E-mail: ikkang@knu.ac.kr.

[†] Department of Polymer Science and Engineering, Kyungpook National University.

[‡] Department of Medical and Biological Engineering, Kyungpook National University.

[§] Korea Institute of Materials Science.

voltage flew to the collector and formed the nanofiber mesh. The polymer solutions were electrospun with a fixed mass flow rate of 1.0 mL/h and a voltage of 15 kV. Finally, the electrospun samples were dried overnight at 40 °C to remove the solvent. The silver-containing PHBV nanofibrous scaffold was named as PHBV/Ag 0.1, PHBV/Ag 0.5, and PHBV/Ag 1.0 depending on the concentration of silver nanoparticles suspension. The morphologies of the electrospun nanofiber were observed by using a field emission scanning electron microscope (FE-SEM S-4300, Hitachi, Japan). The silver nanoparticles embedded in the PHBV nanofiber were observed through a transmission electron microscopy (TEM, H-7600, Hitachi, Japan).

In Vitro Biodegradation. The electrospun PHBV and PHBV/Ag 1.0 nanofibrous scaffolds were cut into rectangles (20 × 20 × 0.05 mm) for in vitro degradation testing. Each specimen was placed in a test tube containing 10 mL of phosphate-buffered saline (PBS, pH 7.0, Gibco) and incubated for 12 h at 37 °C. After incubation, the samples were washed and lyophilized for 24 h. To measure the enzymatic degradation of nanofibrous scaffolds, we incubated the scaffolds in a PBS containing *Pseudomonas stutzeri* BM190 depolymerase (10 mL, 0.05 mg/mL). After incubation for a requisite time (10 min or 1 h), the samples were washed with distilled water and then lyophilized for 24 h. Morphological changes were observed with an FE-SEM.

Antibacterial Assessment. *Staphylococcus aureus* (Gram-positive, SA 6538) and *Klebsiella pneumoniae* (Gram-negative, KP 4352) were cultivated in a nutrient broth for 24 h in a CO₂ incubator. The nanofibrous scaffolds were sterilized in an autoclave and cut into size of 1 × 1 cm². The diluted bacteria suspension was cultured in a vial containing 0.4 g of the samples. The vials were cultured at 37 °C in a shaking incubator for 18 h. The bacteria collected from each vial were plated onto the agar medium. After incubation at 37 °C for 24 h, the resulting bacterial colonies on the plates were counted visually. The percentage of the bacterial growth inhibition was calculated using the difference between the number of colonies from bacteria with samples and that from bacteria in the vial as control. All experiments were performed in triplicate, and the quantitative value was expressed as the average ± standard deviation.

For the inhibition zone test, PHBV and silver-containing PHBV nanofibrous scaffolds were placed on each *Staphylococcus aureus*- and *Klebsiella pneumoniae*-seeded nutrient broth agar plates and incubated overnight at 37 °C. The zone of inhibition against the two microorganisms was analyzed and compared with that of the PHBV control.

Silver Release. The silver release rate could be accelerated because of the biodegradation of PHBV nanofiber in the presence of PHB depolymerase. Therefore, the distilled water was used as the medium for the silver release experiment. The amount of silver nanoparticles released from the sample was conducted by immersing the PHBV/Ag 1.0 (4 × 4 cm², 0.02 g) nanofibrous scaffolds in 10 mL of distilled water (pH 7.2) for different time periods. Then, the concentration of silver in distilled water was determined by inductively coupled plasma spectrophotometer (ICP, Thermo Jarrell Ash IRIS-AP).

Cell Adhesion. To examine the interaction of nanofibrous scaffolds with fibroblast cells (NIH 3T3), the circular nanofibrous scaffolds were fitted in a 24-well culture dish and subsequently immersed in a DMEM medium containing 10% fetal bovine serum (FBS) (Gibco, Japan) and 1% penicillin G-streptomycin (Gibco, Japan). To the scaffolds, 1 mL of the cell solution (3 × 10⁴ cells/cm²) was added to the scaffolds and incubated in a humidified atmosphere of 5% CO₂ at 37 °C for a 4 h. After incubation, the supernatant was removed, washed twice with a PBS, and fixed in a 2.5% glutaraldehyde aqueous solution for 20 min. The sample sheet was then dehydrated, dried in a critical point drier, and finally sputter-coated with gold. The surface morphology of the samples was then observed with a FE-SEM.

Cell Proliferation and Viability. The proliferation of NIH 3T3 cells was determined using a colorimetric immunoassay, enzyme-linked immunosorbent assay (ELISA). This ELISA method is based on the measurement of 5-bromo-2-deoxyuridine (BrdU), which was incorpo-

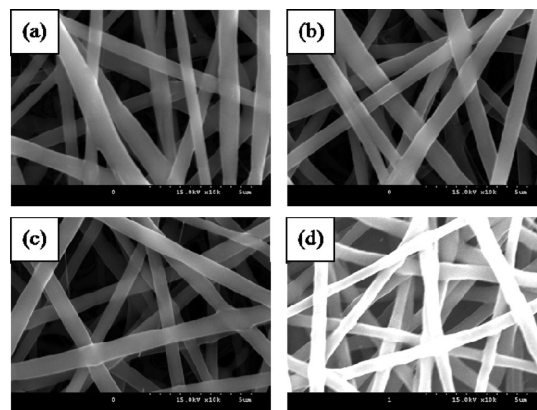


Figure 1. SEM images of (a) PHBV, (b) PHBV/Ag 0.1, (c) PHBV/Ag 0.5, and (d) PHBV 1.0 nanofibrous scaffolds.

rated during DNA synthesis. The ELISA was performed according to the manufacturer's instructions (Roche Molecular Biochemicals).

A standard live/dead assay was used to evaluate cell viability when cultured on the silver-containing PHBV scaffolds. Cells were collected by centrifugation and incubated in calcein-AM (1 mM in PBS) and ethidium homodimer-1 (2.5 mg/mL PBS) solution for 15 min. Cells with compromised membranes exhibit red fluorescence from the live-cell impermeant nucleic acid stain ethidium homodimer-1. Cells with intact cell membranes are able to use nonspecific cytosolic esterases to convert nonfluorescent calcein-AM into bright green-fluorescent calcein. Cells were observed under a fluorescence microscope using a band-pass filter (Nikon Eclipse E600-POL, Japan).

Alkaline Phosphatase Activity. The differentiation of osteoblast cells was evaluated with the expression of alkaline phosphatase (ALP) activity. After 6 and 10 days culture of MC3T3-E1 cells on PHBV and PHBV/Ag 0.5 nanofibrous scaffolds, respectively, ALP staining was performed by a standard procedure according to the manufacturer's instructions (Sigma-Aldrich). After culture, the osteoblast cells were washed with PBS solution and fixed with a citrate-acetone-formaldehyde fixative solution (citrate solution 25 mL, acetone 65 mL, formaldehyde solution 10 mL) at room temperature for 30 s. Subsequently, the cell fixed discs were rinsed three times with PBS solution for 45 s and stained with alkaline-dye mixture (sodium nitrate 1 mL, FBB-alkaline solution 1 mL, naphthol AS-BI alkaline solution 1 mL, deionized water 45 mL) at room temperature for 15 min. After the dye solution was removed, the dyed samples were washed twice with distilled water to remove completely the redundant stains and then dried. The cells stained positively for ALP were observed with an optical microscope (Carl Zeiss, Germany).

The ALP activity of cell lysates was measured according to the method of Ikarashi et al.²¹ The same quantity of 2 mM MgCl₂ in 0.1 M carbonate buffer (pH 10.2) and 20 mM *p*-nitrophenylphosphate were mixed as the substrate solution; then, this substrate solution was preincubated at 37 °C. Cell lysates (20 µL) were incubated with 1 mL of the substrate solution at 37 °C for 30 min. The enzymatic reaction was stopped by the addition of 2 mL of 0.25 N NaOH, and the absorbance of *p*-nitrophenol liberated was read at 410 nm. The calibration curve of ALP activity was made by the standard solutions that diluted calf intestine ALP (Boehringer Mannheim GmbH, Germany) at the various concentrations. Total protein content of cell lysates was measured with minor modification using bovine serum albumin (Wako Pure Chemical Industries) as a reference standard. The ALP activity of cell lysate was normalized for total protein content of the cell lysate.

Results and Discussion

Fiber Morphology. Figure 1 demonstrates SEM images of electrospun nanofibers from 5 wt % PHBV solutions with

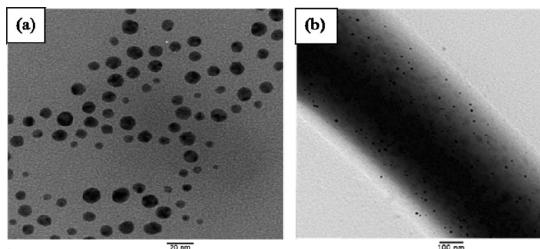


Figure 2. TEM images of (a) free silver nanoparticles and (b) silver nanoparticles distributed to the PHBV nanofibrous scaffolds (PHBV/Ag 1.0).

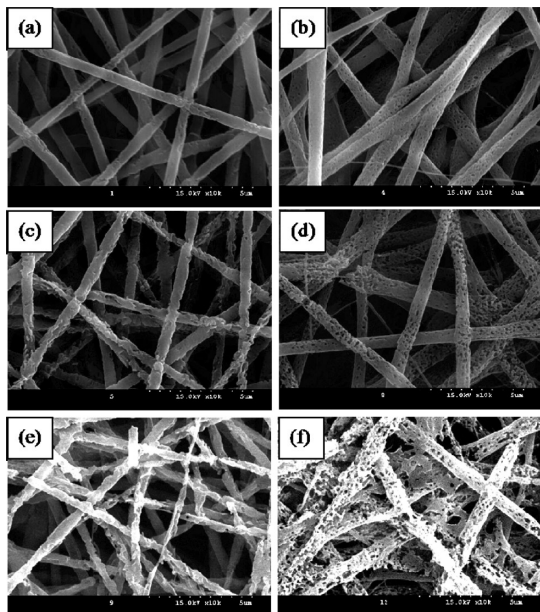


Figure 3. SEM images of (a,c,e) the PHBV and (b,d,f) PHBV/Ag 1.0 nanofibrous scaffolds incubated in PHB depolymerase aqueous for different lengths of time. (a,b) 1 h, (c,d) 6 h, and (e,f) 24 h.

different amounts of silver nanoparticles (0 to 1 wt %). The fiber morphology of PHBV was the same as those of silver-containing PHBVs. However, the average diameter of the electrospun PHBV fibers slightly decreased from 770 ± 40 nm (Figure 1a) to 630 ± 20 nm (Figure 1d) as the silver content increased. This is due to the fact that the conductivity of PHBV solution is proportional to the content of silver.²² The addition of silver enhanced the charge density of PHBV solutions and thus stronger elongation forces were imposed on the ejected jets under the electrical field, resulting in substantially straighter shaped and finer PHBV fibers.^{23,24}

Figure 2 shows the TEM images of free silver nanoparticles and the PHBV/Ag 1.0 nanofibrous scaffold. The diameter of silver nanoparticles used in this study is in the range from 5 to 13 nm, as shown in Figure 2a. The spherical silver nanoparticles were randomly distributed in the PHBV nanofiber (Figure 2b).

Biodegradation. Figure 3 illustrates the morphological changes of the nanofibrous scaffold after incubation in a PBS-containing PHB depolymerase for different time. After 1 h of incubation, surface erosion appeared along the fiber axis of (a) PHBV fibrous scaffold, whereas pores formed on the surface of (b) PHBA/Ag 1.0 scaffold. Erosion of both PHBV and PHBV/Ag 1.0 scaffold increased with an increase in incubation time. However, the erosion rate of PHBV/Ag 1.0 was faster than that of PHBV control. It is considered that the rapid erosion of PHBV/Ag 1.0 is due to the release of silver nanoparticles from the surface and then the biodegradation by PHB depolymerase.

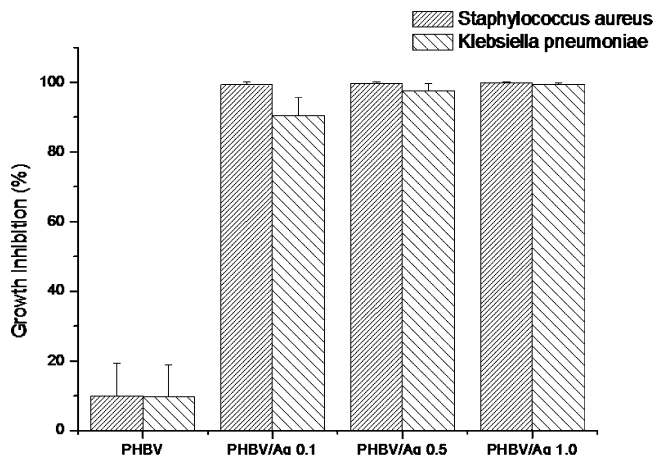


Figure 4. Growth inhibition of PHBV nanofibrous scaffolds with different amounts of silver against *Staphylococcus aureus* and *Klebsiella pneumoniae*.

Antibacterial Activity

The antibacterial capacities of the PHBV/silver nanofibrous scaffolds against Gram-positive *Staphylococcus aureus* and Gram-negative *Klebsiella pneumoniae* were explored by a viable cell-counting method.³ Figure 4 shows the results of the antibacterial tests for the PHBV, PHBV/Ag 0.1, PHBV/Ag 0.5, and PHBV/Ag 1.0 nanofibrous scaffolds against *Staphylococcus aureus* and *Klebsiella pneumoniae*, respectively. As a result, the PHBV nanofibrous scaffold did not show antibacterial activity (<10%). However, the growth inhibition of the PHBV nanofibrous scaffold was markedly enhanced by the addition of silver nanoparticles. PHBV/Ag 0.1 showed 98% growth inhibition against *Staphylococcus aureus* and 90% against *Klebsiella pneumoniae*, and the growth inhibition by PHBV/Ag 0.5 and PHBV 1.0 was reached 99.9% against both Gram-negative and Gram-positive bacteria. These results indicate that the silver nanoparticles are responsible for the antibacterial activity of the composite fibers, and their activity is quite strong. The antibacterial activity of the fiber is attributed to the trace amounts of silver ion released from the fiber, which probably adhered to the negatively charged bacteria and prohibited the growth of bacteria.

Figure 5 shows the effect of the concentration of silver nanoparticles on the formation of zone inhibition. As a result, the silver-containing PHBV nanofibrous scaffolds showed a fair-sized zone of inhibition or region in which the bacterial species refused to propagate around the PHBV/Ag nanofiber scaffold. However, zone inhibition was not formed around the PHBV nanofiber scaffold, showing no antibacterial activity.

The antibacterial activity of the scaffolds is based on the role of silver nanoparticles that were embedded in the surface of nanofiber or released from the surface. Therefore, in this study, the amount of silver nanoparticles released from the PHBV/Ag 1.0 scaffold was calculated using inductively coupled plasma method. As shown in Figure 6, the amount of released silver nanoparticles gradually increased with the increase in incubation time, and it reached 0.557 ppm after 30 days of incubation. Sun et al.²⁴ prepared the Ag-TiO₂ film by a liquid phase deposition method, where the silver nanoparticles were completely trapped in TiO₂ matrix. In their results, the concentration of silver ions released from the Ag-TiO₂ film for 8 days was 0.118 ppm. In this study, the concentration of silver ions released from PHBV/Ag 1.0 nanofibrous scaffold was 0.237 ppm. Rapid release from silver nanoparticles of PHBV/Ag 1.0 is probably

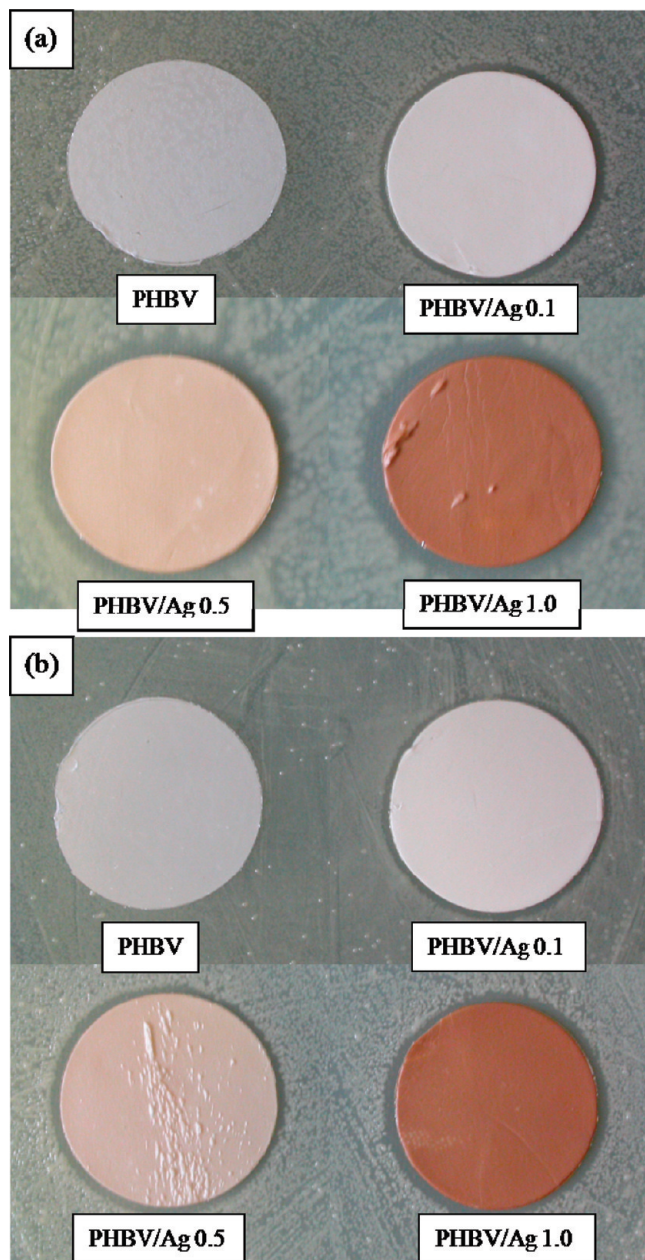


Figure 5. Effect of the concentration of silver nanoparticles on the formation of zone inhibition: (a) *Staphylococcus aureus* and (b) *Klebsiella pneumonia*.

due to the high surface area of the nanofibrous scaffold. The silver nanoparticles released from the nanofibrous scaffold showed high inhibitory effect on the growth of bacteria and killed the microorganisms,²⁵ as shown in Figure 4.

Cytocompatibility

In this study, two kinds of cells (NIH 3T3 fibroblast and MC3T3-E1 osteoblast) were used to test the cytotoxicity of the silver nanoparticles. Fibroblast cells were used to test the cytotoxicity for the shorter incubation time, and the osteoblast cells were used to test the expression of ALP activity for the longer incubation time.

Figure 7 shows NIH 3T3 fibroblasts adhered to the nanofibrous scaffolds. Cells are not fully spread on the scaffolds after 4 h of incubation. A similar result was also reported in the previous work.²⁶ However, the cells are gradually spread as

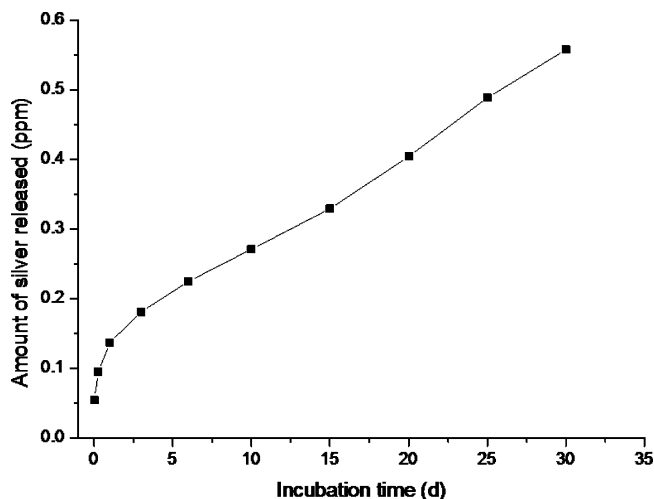


Figure 6. Amount of silver nanoparticles released from PHBV/Ag 1.0 nanofibrous scaffolds as a function of the immersion time.

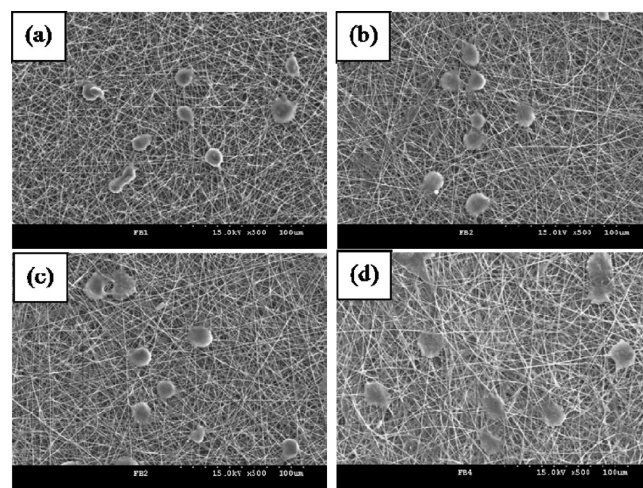


Figure 7. SEM images of NIH 3T3 cells adhered to (a) PHBV, (b) PHBV/Ag 0.1, (c) PHBV/Ag 0.5, and (d) PHBV/Ag 1.0 nanofibrous scaffolds after 4 h of incubation.

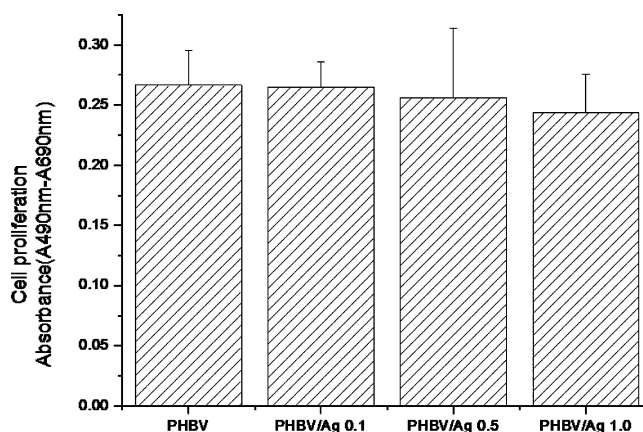


Figure 8. Proliferation of NIH 3T3 cells cultured for 2 days. Data expressed as means \pm SD ($n = 6$) for the specific absorbance.

incubation time increases to 24 h. (Data are not shown here.) Figure 8 shows the proliferation of NIH 3T3 cells cultured for 2 days on the nanofibrous scaffolds. Cell proliferation by the PHBV nanofibrous scaffold is almost the same as that by silver-containing PHBV (PHBV/Ag 0.1, PHBV/Ag 0.5, PHBV/Ag 1.0) within the standard deviation. We observed viability of the cells cultured for 7 days on the PHBV nanofibrous scaffolds by using

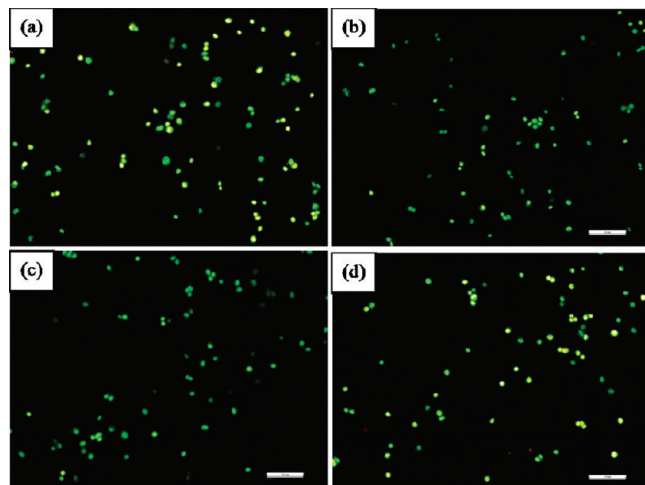


Figure 9. Fluorescence microscopy images of NIH 3T3 cells cultured for 7 days on the (a) PHBV, (b) PHBV/Ag 0.1, (c) PHBV/Ag 0.5, and (d) PHBV/Ag 1.0 nanofibrous scaffolds.

the live/dead assay, and the results are shown in Figure 9. The fluorescence color of cells cultured on the PHBV, PHBV/Ag 0.1, and PHBV/Ag 0.5 scaffolds were totally green, indicating a good viability of the cells. Only a few dead cells showed red fluorescence by the staining of propidium iodide when cultured on the PHBV/Ag 1.0 nanofibrous scaffold (Figure 9d).

ALP activity was determined to be an indicator of osteoblastic differentiation of MC3T3-E1 cultured on PHBV and PHBV/Ag 1.0 nanofibrous scaffolds.²⁷ As shown in Figure 10, the ALP activities of the cells on PHBV and PHBV 1.0 nanofibrous scaffold increased with the increase in incubation time. The degree of ALP activity expressed by PHBV scaffold was not significantly different from that by PHBV/Ag 1.0 for 10 days (Figure 10e).

Haimi et al²⁸ fabricated three types of bioactive glass scaffolds (nontreated, thick, and thin Ca–P treated) and reported that the ALP activity of the cells cultured for 1 week on nontreated bioactive glass scaffolds was significantly higher than that of those cultured on both thin and thick Ca–P-treated scaffolds. However, these differences equalized between the three scaffolds by the 2-week time point. Therefore, they concluded that osteogenic differentiation appears to be delayed on the Ca–P surface-treated scaffolds. Ge et al²⁹ prepared the 3D poly-(lactic-co-glycolic acid) (PLGA) scaffolds and reported that ALP activity expressed by the osteoblasts cultured on the PLGA scaffolds was almost the same as that on the open-cell polylactic acid (OPLA) and collagen scaffolds (Becton-Dickinson, Franklin Lakes, NJ). They concluded that the PLGA scaffold can support the proliferation of osteoblasts as well as the expression of genes, which is important for osteogenesis such as ALP, osteocalcin, collagen I, and osteopontin. The PHBV is a natural polyester polymerized by bacteria. The PHBV is biological origin and environmentally more acceptable. In this study, it is considered that both PHBV and silver-containing PHBV nanofibrous scaffolds can support the expression of genes important for osteogenesis (ALP activity).

The question is often raised of why silver does not have cytotoxic effects on eukaryotic cells. Eukaryotic cells are usually larger than prokaryotic cells and exhibit a far bigger target for attacking silver ions. Eukaryotic cells also show higher structural and functional redundancy compared with prokaryotic cells; therefore, higher silver ion concentrations are required to achieve comparable toxic effects than for bacterial cells.³⁰ This differ-

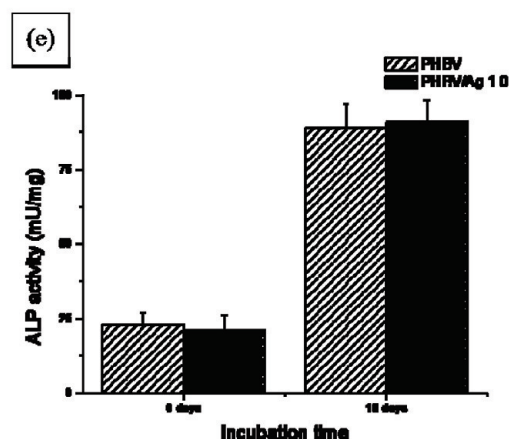
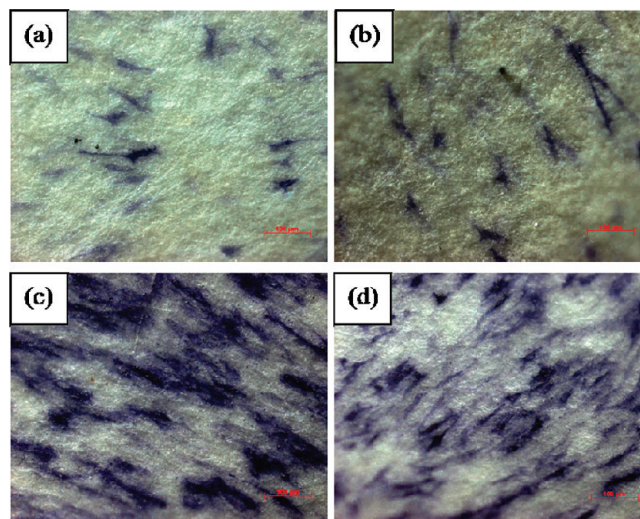


Figure 10. Alkaline phosphatase (ALP)-stained (a) PHBV, (b) PHBV/Ag 1.0 nanofibrous scaffolds after 6 days of incubation of MC3T3-E1 osteoblasts, and (c) PHBV, (d) PHBV/Ag 1.0 nanofibrous scaffolds after 10 days incubation of MC3T3-E1 osteoblasts, and (e) ALP expression of MC3T3-E1 osteoblasts on the nanofibrous scaffolds.

ence makes it possible that the bacterial cells are successfully attacked by the silver ions, whereas harmful effects on eukaryotic cells cannot yet be observed. As reported in this study, no cell cytotoxicity with a high antibacterial activity against *Staphylococcus aureus* and *Klebsiella pneumoniae* was observed for PHBV nanofibrous scaffolds having silver nanoparticles <1.0 wt %.

Conclusions

Silver-containing PHBV nanofibrous scaffolds were successfully prepared via an electrospinning technique and were characterized by SEM and TEM. The results demonstrated that the nanofibers electrospun under maximum conditions were straight, and silver nanoparticles were randomly distributed to the surface of the fibers. Finally, the PHBV nanofibrous scaffolds having silver nanoparticles <1.0 wt % (PHBV/Ag 0.1 and PHBV/Ag 0.5) completely inhibited the proliferation of *Staphylococcus aureus* (Gram-positive) and *Klebsiella pneumoniae* (Gram-negative) bacteria, whereas the scaffolds did not show in vitro cell cytotoxicity. If these results can be further confirmed in vivo, then the silver-containing PHBV nanofibrous scaffolds may have a high interest in total joint arthroplasty, particularly because of their effect against multiresistant bacteria.

Acknowledgment. This research was supported by the research grants of the Biotechnology development project (2009-0090907) from the Ministry of Science and Technology of Korea.

References and Notes

- (1) Fauci, A. S.; Touchette, N. A.; Folkers, G. K. *Emerging Infect. Dis.* **2005**, *11*, 519–525.
- (2) Sonodi, I.; Salopek-Sondi, B. *J. Colloid Interface Sci.* **2004**, *275*, 177–182.
- (3) Taylor, P. L.; Ussher, A. L.; Burrell, R. E. *Biomaterials* **2005**, *26*, 7221–7229.
- (4) Chambers, C. W.; Proctor, C. M.; Kabler, P. W. *J.-Am. Water Works Assoc.* **1962**, *54*, 208–216.
- (5) Berger, T. J.; Spadaro, J. A.; Bierman, R.; Chapin, S. E.; Becker, R. O. *Antimicrob. Agents Chemother.* **1976**, *10*, 856–860.
- (6) Kusnetsov, J.; Iivanainen, E.; Elomaa, N.; Zacheus, O.; Martikainen, P. *J. Water Res.* **2001**, *35*, 4217–4225.
- (7) Russell, A. D.; Hugo, W. B. *Prog. Med. Chem.* **1994**, *31*, 351–370.
- (8) Crede, K. S. F. *Die Verhütung der Augenentzündung der Neugeborenen, der häufigsten und wichtigsten Ursache der Blindheit.* A. Hirschwald: Berlin, 1884.
- (9) Wyatt, D.; McGowan, D. N.; Najarian, M. P. *J. Trauma* **1990**, *30*, 857–865.
- (10) Bechert, T.; Steinrucke, P.; Guggenbichler, J. P. *Nat. Med.* **2000**, *6*, 1053–1056.
- (11) Jensen, E. L.; Rungby, J.; Hansen, J. C.; Schmidt, E.; Pedersen, B.; Dahl, R. *Hum. Toxicol.* **1988**, *7*, 535–540.
- (12) König, O.; Randerath, O.; Hackenbroch, M. H. *Unfallchirurg* **1999**, *102*, 324–328.
- (13) Williams, S. F.; Martin, D. P.; Horowitz, D. M.; Peoples, O. P. *Int. J. Biol. Macromol.* **1999**, *25*, 111–121.
- (14) Hocking, P. J.; Marchessault, R. H. *Chemistry and technology of biodegradable polymers.* Blackie Academic and Professional: New York, 1994.
- (15) Xu, X.; Yang, Q.; Wang, Y.; Yu, H.; Chen, X.; Jing, X. *J. Eur. Polym. J.* **2006**, *42*, 2081–2087.
- (16) Park, S. J.; Jang, Y. S. *J. Colloid Interface Sci.* **2003**, *261*, 238–243.
- (17) Yeo, S. Y.; Lee, H. J.; Jeong, S. H. *J. Mater. Sci.* **2003**, *38*, 2143–2147.
- (18) Park, S. W.; Bae, H. S.; Xing, Z. C.; Kwon, O. H.; Huh, M. W.; Kang, I. K. *J. Appl. Polym. Sci.* **2009**, *112*, 2320–2326.
- (19) Kim, C. N.; Xing, Z. C.; Baek, J. Y.; Bae, H. S.; Kang, I. K. *Polymer (Korea)* **2009**, *33*, 429–434.
- (20) Lee, K. H.; Kim, H. Y.; Ryu, Y. J.; Kim, K. W.; Choi, S. W. *J. Polym. Sci., Part B: Polym. Phys.* **2003**, *41*, 1256–1262.
- (21) Ikarashi, Y.; Tsuchiya, T.; Nakamura, A. *Biomaterials* **2000**, *21*, 1259–1267.
- (22) Ohkawa, K.; Minato, K. I.; Kumagai, G.; Hayashi, S.; Yamamoto, H. *Biomacromolecules* **2006**, *7*, 3291–3294.
- (23) Son, W. K.; Youk, J. H.; Lee, T. S.; Park, W. H. *Polymer* **2004**, *45*, 2959–2966.
- (24) Zong, X.; Kim, K.; Fang, D.; Ran, S.; Hsiao, B. S.; Chu, B. *Polymer* **2002**, *43*, 4403–4412.
- (25) Sun, S. Q.; Sun, B.; Zhang, W. Q.; Wang, D. *Bull. Mater. Sci.* **2008**, *31*, 61–66.
- (26) Yuan, J.; Xing, Z. C.; Park, S. W.; Geng, J.; Kang, I. K. *Macromol. Res.* **2009**, *17*, 850–855.
- (27) Isama, K.; Tsuchiya, T. *Biomaterials* **2003**, *24*, 3303–3309.
- (28) Haimi, S.; Moimas, L.; Pirhonen, E.; Lindroos, B.; Huhtala, H.; Raty, S.; Kuokkanen, H.; Sandor, G. K.; Miettinen, S.; Suuronen, R. *J. Biomed. Mater. Res., Part A* **2009**, *91*, 540–547.
- (29) Ge, Z.; Wang, L.; Heng, B. C.; Tian, X. F.; Lu, K.; Fan, V. T. W.; Yeo, J. F.; Cao, T.; Tan, E. *J. Biomater. Appl.* **2009**, *23*, 533–547.
- (30) Alt, V.; Bechert, T.; Steinrucke, P.; Wagener, M.; Seidel, P.; Dingeldein, E.; Domann, E.; Schnettler, R. *Biomaterials* **2004**, *25*, 4383–4391.

BM1000372